10-15-2023

Thermodynamic properties of common salts in aqueous solutions

Li Shu
Edith Cowan University

Veeriah Jegatheesan

Leonardo Jegatheesan

10.1016/j.desal.2023.116797
Shu, L., Jegatheesan, V., & Jegatheesan, L. (2023). Thermodynamic properties of common salts in aqueous solutions. Desalination, 564, article 116797. https://doi.org/10.1016/j.desal.2023.116797

Desalination 564 (2023) 116797

Contents lists available at ScienceDirect

Desalination

journal homepage: www.elsevier.com/locate/desal

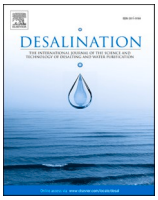

Thermodynamic properties of common salts in aqueous solutions

Li Shu [a,*], Veeriah Jegatheesan [b], Leonardo Jegatheesan [c]

[a] School of Engineering, Edith Cowan University, 70 Joondalup Drive, Joondalup, Perth, WA 6027, Australia
[b] School of Engineering, RMIT University, 402 Swanston Street, Melbourne, VIC 3000, Australia
[c] School of Psychology, Adelaide University, 259 North Terrace, Adelaide, SA 5000, Australia

HIGHLIGHTS

- Proton and hydrogen-ion activities linked by an equation.
- System's negative potential energy = proton activity × electrostatic potential
- Negative potential energy is equal to the Gibb's energy.
- pH values yield key thermodynamic properties.
- Negative entropy indicated the orderly nature of a system.

ARTICLE INFO

Keywords:
Aqueous solution
Common salt
Charge activity
pH
Potential energy

ABSTRACT

A relationship between the activity of hydrogen ions and charge activity in an aqueous solution has been developed in a previous study. That study also revealed that the potential energy of an aqueous solution can be obtained by multiplying the charge activity with electrostatic potential of the solution. In this study, negative potential energy equalling Gibbs energy of four common salt (NaCl, KCl, $NaNO_3$ and KNO_3) solutions were quantified using the charge activity. Then the entropies of those salt solutions were computed using the Gibbs energy, enthalpy, and the charge activity. Charge activities were computed using the pH of those solutions at room temperature. It was found that potential energy, Gibbs energy, enthalpy and entropy of a solution is related to the charge activity of a solution, not the ionic charge number as previously thought. When the concentrations of NaCl, KCl, $NaNO_3$ and KNO_3 increased in single solutions the entropies of those solutions tend to decrease allowing them to achieve orderly states leading the salt particles to crystalise. The findings of this study will lead to better understanding and utilization of thermodynamic properties during crystallization which is vital important in brine recovery.

1. Introduction

The world is facing a growing water shortage crisis due to the increase in population. One of the effective ways to provide fresh water is through seawater desalination. However, the process of reverse osmosis used in desalination generates concentrated steam or brine which is mostly discharged into the ocean, causing environmental degradation [1–4]. Therefore, it is necessary to have sustainable brine management [5–10].

Extensive research is currently focused on various aspects of seawater brine generated by reverse osmosis (RO) and nanofiltration (NF) processes. The objective is to enhance water and salt recovery while minimizing energy consumption, thus establishing seawater desalination as a sustainable solution to alleviate water scarcity worldwide.

For instance, researchers are exploring the synthesis of magnesium sulfate from seawater, employing alkaline industrial wastes, sulfuric acid, and organic solvents [11]. Additionally, cationic selectrodialysis is being extensively studied for magnesium recovery from seawater [12]. The selectivity of divalent and monovalent ions plays a crucial role in improving the performance of NF/RO systems for desalination. This improved performance leads to enhanced water recovery and the production of pure $MgSO_4$ and NaCl salts.

To achieve this, several studies have investigated factors such as the

* Corresponding author.
E-mail address: li.shu846@gmail.com (L. Shu).

https://doi.org/10.1016/j.desal.2023.116797
Received 15 March 2023; Received in revised form 2 June 2023; Accepted 19 June 2023
Available online 22 June 2023

permselectivity of divalent and monovalent cations under different applied current densities and ionic species concentrations [13]. Moreover, the development of amphoteric blend ion-exchange membranes for separating monovalent and divalent anions in electrodialysis has been explored [14]. The ideal selectivity and performance of selectrodialysis using thin-film composite (TFC) ion exchange membranes have also been investigated [15]. Selective electrodialysis has been studied for the separation of monovalent and divalent ions from seawater reverse osmosis brine [16]. Other research includes ion fractionation and metathesis through an integrated system of nanofiltration and electrodialysis to improve water recovery [17], as well as fractionating magnesium ions from seawater for struvite recovery using electrodialysis with monovalent selective membranes [18]. These studies contribute to the development of highly permselective NF membranes.

Furthermore, studies are underway to optimize sequential CO_2 mineralization using seawater desalination brine [19], explore CO_2 utilization through conjoined electrolysis using desalinated rejected seawater brine [20], and investigate seawater bittern recovery processes for CO_2 and SO_x utilization [21]. These endeavours aim to contribute to climate change mitigation by promoting carbon capture. Comprehensive understanding and exploration of resource recovery from seawater desalination brine are being pursued through review and experimental studies, including laboratory and pilot-scale investigations [22]. Valuable information on resource recovery has been gleaned, such as the recovery of Na_2SO_4 crystals [23], reclamation of concentrated brine from RO plants using selectrodialysis with bipolar membranes [24], calcium sulfate recovery [25], recovery of reactive MgO through the addition of NaOH [26], removal of magnesium as a pre-treatment for membraneless electrolysis [27], recovery of magnesium hydroxide [28], sodium hydroxide [29,30], and boron by selective ion exchange resins [31]. Moreover, studies on ammonium recovery using thin film composite forward osmosis membranes employing tris(2-aminoethyl) amine [32] offer insights into the recovery of valuable resources through hybrid membrane processes. Collectively, these ongoing investigations demonstrate the commitment to advancing our knowledge and capabilities in resource recovery and sustainable practices within the realm of seawater desalination brine.

Recently, there has been a focus on recovering valuable metals [33-47] from the discharged concentrate brine. Extensive research is underway to explore various methods for lithium recovery, considering its increasing value for diverse applications. These methods include the utilization of ion-exchange resins [33], both homogenous and heterogeneous precipitation techniques [34], heterogenous ion exchange with bipolar membrane electrodialysis (BMED) [36], flow-type electrochemical lithium recovery (ELR) systems [37,39], modified membrane capacitive deionization systems [40], closed-loop processes involving electrochemical methods and precipitation [41], as well as the investigation of novel precipitants. The significance of lithium as a valuable resource has prompted comprehensive studies in these areas. Researchers are actively examining the extraction of rubidium from seawater brine, employing integrated membrane distillation-selective sorption systems [42] and other innovative methods [46]. Furthermore, nanofiltration techniques are being explored for the recovery of indium and germanium from bioleaching solutions [45]. These extensive research efforts signify the growing importance of lithium and other valuable elements, driving the exploration of novel and efficient recovery methods. The advancements in these areas hold significant potential for resource sustainability and meeting the increasing demand for these valuable materials.

It is important to have full-scale production of mineral mining from concentrates [48], and ultimately achieve zero liquid discharge [49–51]. In addition, understanding the thermodynamic properties of element separation during mineral mining is crucial [52–54]. Thermodynamic properties such as enthalpy and entropy are important factors which need to be understood well to optimize the crystallization. For example, studies have found that water-salt permeability to be entropically driven and ion-ion selectivity is limited due to an enthalpy-entropy compensation [54]. Further, Gibb's energy is used to evaluate the extraction capacities of adsorbents that are used to adsorb various cations present in seawater desalination brine [52]. Thus, the aim of this study was to investigate the thermodynamic properties of four common salts in aqueous solutions at room temperature, using their pH values.

1.1. Thermodynamic properties of aqueous solutions

Sørensen defined pH as $pH = -\log(a_{H+})$, where $a_{H+} = c_{H+}/c_o$, c_{H+} is the hydrogen concentration ($[H^+] = c_{H+}$), and c_o is the standard state hydrogen ion concentration, which is 1 mol/L [55].

Since one hydrogen ion possesses one proton, we can write $[H^+] = [e^+]$, where e^+ is the proton concentration, with unit mole per litre. Dividing both sides of the equation by c_o gives:

$$a_{H+} = v \tag{1}$$

Where v is the proton activity. It is obtained from $v = c_{e+}/c_o$, c_{e+} is the concentration of proton. Since $pH = -\log(a_{H+})$ and $a_{H+} = v$, we can have,

$$pH = -log(v) \tag{2}$$

$$v = 10^{-pH} \tag{3}$$

$$-v = 10^{pH-14} \tag{4}$$

Where -v is the activity of electrons [56]. Column 1 and 2 in Table 1 can be constructed using the relationship between the pH and charge activities.

Electrostatic potential (E_{cell}) is computed using E_{cell} (mV) = 414.12–59.16pH shown in Fig. 1 [56]. E_{cell} is the electrostatic potential measured using a pH meter.

Potential energy is calculated as $vE_{cell}F$ [56], which will always be positive value in Table 1 since positive charge will have positive electrostatic potential and negative charge will have negtive E_{cell} values.

Nernst equation relates the electrical properties of solutions to their chemical properties, and it is written as follow [57].

$$E_{cell}\ (mV) = E^o{}_{cell} - RT\ lnQ/nF \tag{5}$$

Where, as mentioned previously, E_{cell} is the electrostatic potential

Table 1
Electrical and thermodynamic properties of solutions with different pH at 25 °C.

pH	ν/a_{H+}	E_{cell} mV	$-\nu FE_{cell}/\nu\Delta G_{cell}$ mJ/mol	$-\nu FE^o_{cell}/\nu\Delta G^o_{cell}$ mJ/mol	$\nu\Delta_rG/RTln[Q]$ mJ/mol
0	1	414.12	-4.00×10^7	-4.00×10^7	0
1	0.1	354.96	-3.42×10^6	-4.00×10^6	-5.71×10^5
2	0.01	295.80	-2.58×10^5	-4.00×10^5	-1.14×10^5
3	0.001	236.64	-2.28×10^4	-4.00×10^4	-1.71×10^4
4	10^{-4}	177.48	-1.71×10^3	-4.00×10^3	-2.28×10^3
5	10^{-5}	118.32	−114.16	−399.57	−285.42
6	10^{-6}	59.16	−5.71	−39.96	−34.25
7	10^{-7}	0	0	−4.00	−4.00
8	-10^{-6}	−59.16	−5.71	39.96	45.67
9	-10^{-5}	−118.32	−114.16	399.57	513.75
10	-10^{-4}	−177.48	-1.71×10^3	4.00×10^3	5.71×10^3
11	−0.001	−236.64	-2.28×10^4	4.00×10^4	6.28×10^4
12	−0.01	−295.80	-2.85×10^5	4.00×10^5	6.85×10^5
13	−0.1	−354.96	-3.42×10^6	4.00×10^6	7.42×10^6
14	−1	−414.12	-4.00×10^7	4.00×10^7	7.99×10^7

$pH = -\log[a_{H+}]$; $v = [a_{H+}]$; At 25 °C, E_{cell} (mV) = 414.12–59.16pH; F is Faraday constant.
$-vE_{cell}F = v\Delta G_{cell}$; At 25 °C, $\Delta G^o_{cell} = -4.00 \times 10^{-7}$ mJ/mol; R is gas constant, T is temperature in Kelvin; When we measure pH instead of products and reactants of a reaction we let $[Q] = [a_{H+}]$.

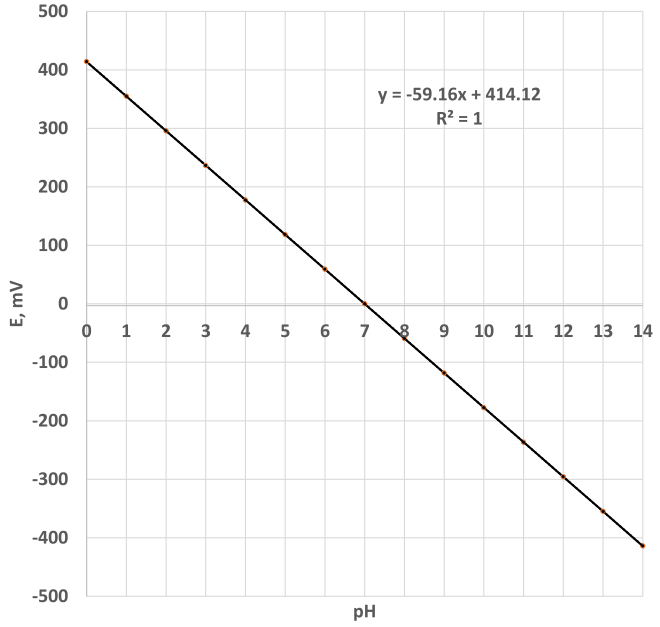

Fig. 1. Relationship between pH and electrostatic potential (mV) at 25 °C.

measured using a pH meter; E^{o}_{cell} is the standard cell/electrostatic potential; R is gas constant; T is temperature in Kelvin; Q is a reaction quotient, which is the multiplication of the molar concentrations of products raised to the powers of their respective stoichiometric coefficients divided by the multiplication of the molar concentrations of the reactants raised to the powers of their respective stoichiometric coefficients in a reaction, (for example in a reaction of aA + bB ⇌ cC + dD then $Q = [C]^c[D]^d/([A]^a[B]^b)$; F is Faraday constant; n is ionic charge number and $n = 1$ is used in the following calculations.

When we measure pH instead of products and reactants of a reaction we let

$$[Q] = [a_{H+}] \tag{6}$$

The standard cell potential is defined as

$$E^{o}{}_{cell} = -\Delta_{cell}G^{o}/nF \tag{7}$$

$$\text{and } E_{cell} = -\Delta_{cell}G/nF \tag{8}$$

When Eqs. (7) and (8) are substituted into Eq. (5), we have.

$$\Delta_{cell}G = \Delta_{cell}G^{o} + RTlnQ \tag{9}$$

Eq. (9) shows the reaction Gibbs energy at an arbitrary stage [57].

In thermodynamics, it assumed that the standard Gibbs energy for the formation of hydrogen is zero at all temperature, Δ_fG^o, $(H^+) = 0$, where the subscript "f" represents formation. So, for the physical reaction of salt dissolution in water, $\Delta_rG = \Delta_rG^o + RTln[Q]$, where the subscript 'r' means reaction. When $\Delta_rG^o = 0$, we have

$$\Delta_rG = RTln[Q] = 2.3RTlog[a_{H+}] = -2.3RT{\cdot}pH \tag{10}$$

Comparing Eq. (10) with Eq. (9), we have.

$$\Delta_{cell}G = \Delta_{cell}G^{o} + \Delta_rG \tag{11}$$

Values of $\Delta_{cell}G$, $\Delta_{cell}G^o$ and Δ_rG are listed on columns 4 to 6 in Table 1. Their values are computed according to modified Eqs. (7), (8) and (10):

$$vE_{cell}F = -v\Delta_{cell}G \tag{12}$$

$$vE^{o}{}_{cell}F = -v\Delta_{cell}G^{o} = -414.16vF \tag{13}$$

$$v\Delta_rG = -2.3vRT{\cdot}pH = -5.71 \times 10^{6}v{\cdot}pH \tag{14}$$

The above three equations recognize the energy potential of a solution is related to its charge activity instead of ionic charge number and are developed in this study and used first time.

As mentioned previously, $\Delta_{cell}G$ means the values obtained from pH measurement and Δ_rG is obtained assuming the standard Gibbs energy for forming hydrogen ions equals to zero.

In thermodynamics, it is defined that $\Delta G = \Delta H - T\Delta S$ and we therefore can have.

$$\Delta_{cell}G = \Delta_{sol}H - T\Delta S \tag{15}$$

Where $\Delta_{sol}H$ is enthalpy. The change in enthalpy is equal to the energy supplied as heat at constant pressure (provided the system does no additional work). Enthalpy is generally measured by monitoring temperature change during a reaction using a calorimeter [57]. $\Delta_{sol}H$ will be positive values if a chemical or physical reaction absorbs heat and it will be negative if the reaction releases heat. ΔS is entropy, whose unit is J/mol. The entropy is an indicator of the chaotic state of a system and when it is negative the system becomes orderly.

2. Materials and methods

2.1. Research materials

Analytical grade salts, potassium chloride (KCl), potassium nitrate (KNO_3), sodium chloride (NaCl) and sodium nitrate ($NaNO_3$), are used during the experiments. Demineralized water (DI water) is used to make solutions. Its pH is around 5.70.

2.2. Research method

pH measurement was carried out according to the instruction from the manufacturer of the pH meter. pH meter is calibrated before measurements at the beginning of each day. The pH meter has an error 7 ± 0.02. Each sample is measured at least twice, and the average value is taken. Solutions are mixed thoroughly. Saturated solutions are allowed for precipitate to settle after mixing. pH of supernatant is measured only. The Kimwipes, a kind of lint less tissue paper, is used to clean the pH meter.

2.3. Research condition

The laboratory is a wet laboratory, and the room temperature is 22 ± 2 °C.

3. Results and discussions

pH of four kinds of common salt solutions were measured and the results are shown in Fig. 2 a). pH values increase with salt concentration for all four kinds of salt solutions, which matches the results from previous studies [58]. Among them, pH of NaCl solution increases the most. It is from 6.16 pH unit at a concentration of 0.0001 M to 8.58 at 5 M, which is 2.42-unit increment. Around 2.2 M, pH of NaCl solution is 7. $NaNO_3$ has the second highest pH increase. It is 5.71 at 0.0001 M and 7.28 at 5 M. It is 1.57-unit increase. pH of $NaNO_3$ solution is 7 at around 4.4 m. For KCl, its pH is 5.62 at 0.0001 M and 6.43 at 6 M. The increment is 0.81 unit. KNO_3 has the least pH increment. Its pH is 5.53 at 0.0001 M and 5.74 at 6 M. The increment of pH is 0.21 unit. All the pH values of both potassium salts are <7 with the salt concentration up to 6 M. It is noticed that some pH values of salt solutions are lower than those of DI water's (pH of DI water is around 5.70), e.g., both potassium sats at 0.0001 M. One explanation is that when salt dissolving in water it causes water clusters to shrink [59]. Water is acidic at pH 5.7. After shrink, its surface area becomes smaller and charge density becomes larger so that solution becomes more acidic. This showed that at low salt concentration, water contributes more to the solution pH while salts dominate the

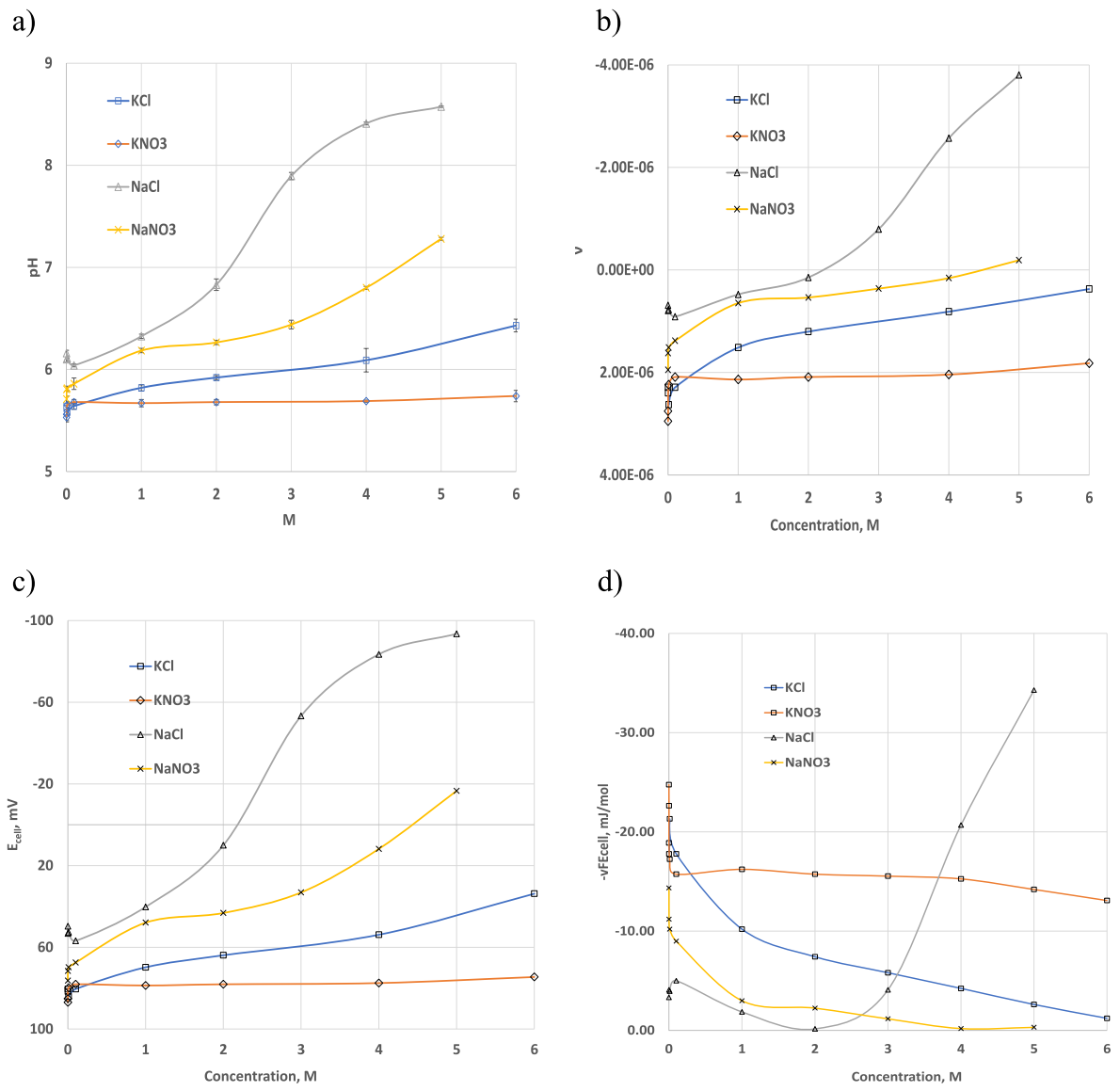

Fig. 2. pH and other electrical properties of common salts.

pH at higher salt concentrations. In other words, charge activity at higher salt concentrations is mainly from salts, which have no hydrogen ions but cations and anions. The fact of the pH of four kinds of potassium salt solutions increasing with concentration shows that they are basic salts.

Charge activity is shown in Table 1. At pH 7, the charge activity has its lowest value 10^{-7}. Charge activity is positive when pH <7 and negative when pH >7. This means that when pH <7, solutions are positively charged, and cations are dominant. At pH >7, solutions are negatively charged, and anions are dominant. With every pH unit decrease from pH 7, the charge activity increases 10 times. At pH 0, charge activity equal 1. Ionic charge number, n, and charge activity can be equal only at pH = 0 where n and ν equals to 1 ($n = \nu = 1$). For calculating potential energy, we use the value of charge activity instead of ionic charges number.

Charge activity of four kinds of salt solutions is shown in Fig. 2 b). We can see that NaCl solutions have the least proton activity, which is 6.92×10^{-7} at 0.0001 M. It becomes negative from 3 M, which is -7.96×10^{-7} and at 5 M, it is -3.80×10^{-7}. Its proton activity decreases as salt concentration increases. Less proton or positive charge activity means more electrons or negative charge activity. So that the pH of NaCl solution increases and electron activity increase. Charge activity of $NaNO_3$ solution decreases from 1.95×10^{-6} at 00001 M to -1.91×10^{-7} at 5 M. For KCl solution its charge activity is 2.40×10^{-6} at 00001 M to 3.72×10^{-7} at 6 M. Charge activity of KNO_3 solution decreases from 2.95×10^{-6} at 00001 M to 1.82×10^{-6} at 6 M. Like NaCl, pH and electron activity of the other three common salt solutions increase with salt concentration.

pH related to electrostatic potential at 25 °C follows the equation: E_{cell} (mV) = 414.12–59.16pH and its values are shown in Fig. 2 c). NaCl solution has the lowest electrostatic potential (E_{cell}) at 0.0001 M, which is 49.69 mV. E_{cell} decreases with concentration until 2 M. At 3 M, it becomes negative value (−53.24 mV). At 5 M, E_{cell} is −93.47 mV. E_{cell} = 0 at around 2.2 M for NaCl solution. $NaNO_3$ solutions has the second lowest E_{cell} at 0.0001 M. It is 76.32 mV at 0.0001 M and − 16.56 mV at 5 M. Both E_{cell} values of KCl and KNO_3 decrease with concentration. At 0.0001 M E_{cell} of KCl solution is 81.64 mV and 33.72 at 6 M while E_{cell} values of KNO_3 solutions are 86.97 mV at 0.0001 M and 74.54 mV at 6 M.

Potential energy $-\nu FE_{cell}$ or $\nu\Delta G_{cell}$ are list in Table 1. They are all negative values since for positively charged solutions, their electrostatic potentials have also positive values and vice versa. $\nu\Delta G_{cell}$ <0 means

that all the salt dissolution studied happens spontaneous, which matches our experimental observations.

Values of energy potential, $-\nu FE_{cell}$, for the four kinds of common salts are in Fig. 2d). The negative energy potential of NaCl solution first decreased then increased from around 2 M while negative energy potentials for other three salt solutions decreased with concentrations. At concentration <2 M, NaCl has the lowest negative potential or Gibbs energy. It has less tendency to dissolve in water than other 3 kinds of salt. At 3 M, its negative potential overtakes that of KNO_3 and at 4 M, NaCl has the highest negative potential value. This shows that salt solutions of positively charged will have less potential/tendency to dissolve in water when the concentration increases while negatively charged salt solutions, such as NaCl >4 M, can have higher ability to dissolve in water, however, the higher dissolution will stop at the saturation point.

In Table 1, we could see that values of both $\Delta_{cell}G^o$ and Δ_rG or RTln[Q] have different signs. They are positive with pH <7 and negative when pH >7.

Both standard Gibb energy, $\nu\Delta_{cell}G^o$, and Gibbs energy, $\nu\Delta_rG$, of the salt solutions are depicted in Fig. 3 a) and b). $\nu\Delta_{cell}G^o$ plus $\nu\Delta_rG$ are also depicted in Fig. 3 c). We predict that negative energy potential in Fig. 2 d) should have the same trend as Fig. 3 c). However, they are different, so we plotted $\nu\Delta_{cell}G^o$ minus $\nu\Delta_rG$ instead and depicted in Fig. 3 d). Both d) drawings in Fig. 3 and Fig. 2 are exactly the same so that the right equation for Gibbs energy should be,

$$\Delta_{cell}G = \Delta G^o{}_{cell} - RTlnQ \quad (16)$$

If we do a calculation using Table 1, we get the same equation $\Delta_{cell}G^o = \Delta G^o_{cell} - RTlnQ$. Consequently, Eq. (5) should be E_{cell} (mV) $= E^o_{cell} + RTlnQ/nF$ instead of E_{cell} (mV) $= E^o_{cell} - RTlnQ/nF$. From Table 1 we notice that when pH = 0, v = 1 and $\nu\Delta G^o_{cell} = -4.00 \times 10^7$ mJ/mol and RTln[Q] = 0. For every solution, we can measure its pH at certain temperatures. We can get its values of $\nu\Delta_{cell}G^o$, $\nu\Delta G^o_{cell}$ and RTln[Q] easily with a pH meter, therefore, pH meter is not only an important and convenient tool measuring solution pH but also a powerful instrument to explore the electrical and thermodynamic properties of solutions.

Table 2
Enthalpy of solution of electrolytes [57].

Solute	State	$\Delta_{sol}H$, kJ/mol	Solute	State	$\Delta_{sol}H$, kJ/mol
KCl	crystal	17.22	NaCl	crystal	3.88
KNO_3	crystal	34.89	$NaNO_3$	crystal	20.50

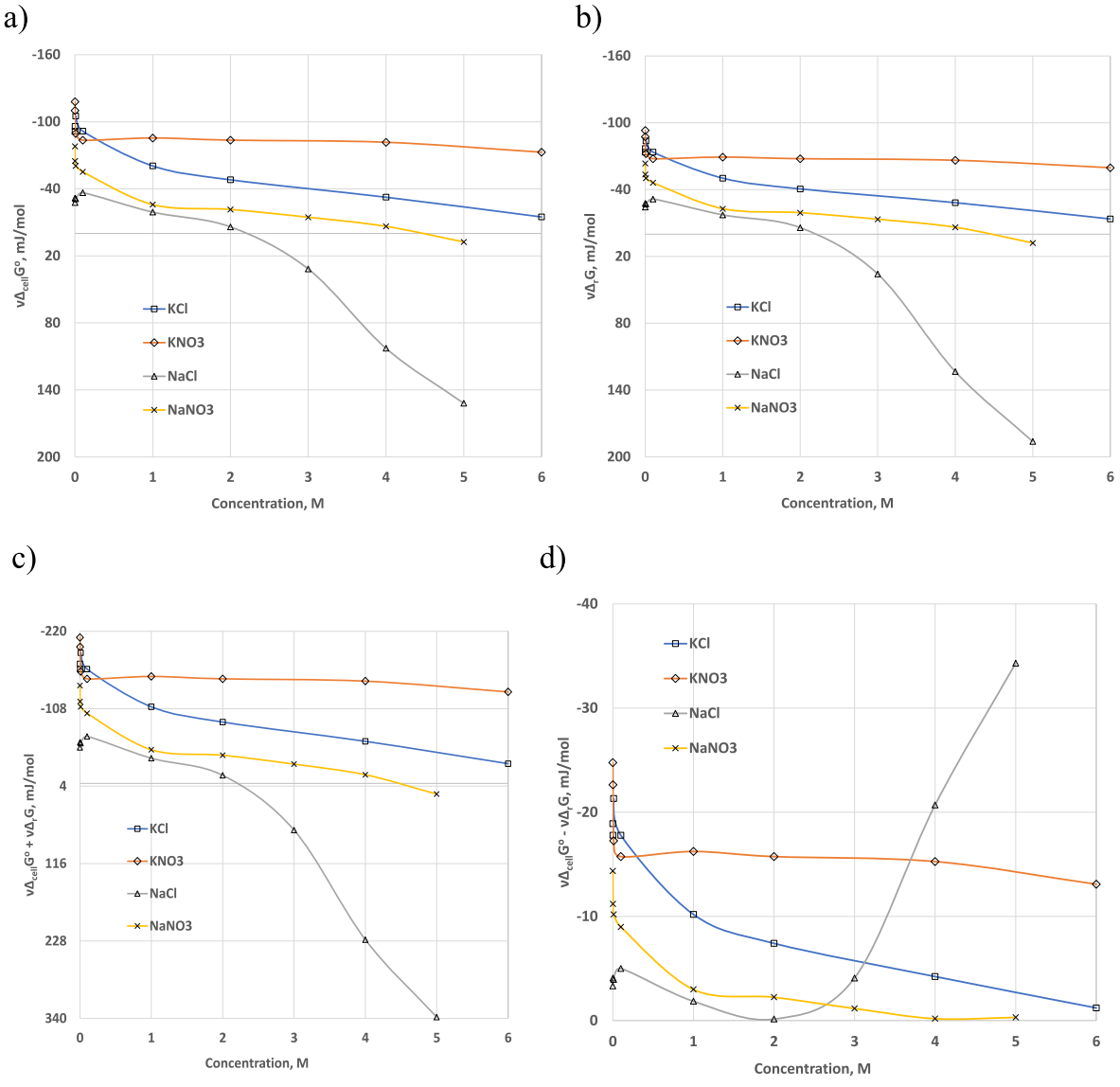

Fig. 3. Standard Gibbs energy and Gibbs energy of common salt solutions.

The molar enthalpy of four kinds of common salt solutions is given in Table 2. It is the enthalpy change when 1 mol of solute in its standard state is dissolved in an infinite amount of water. Values are given in kilojoules per mole at 25 °C [57]. The product of charge activity and enthalpy (heat), $\nu\Delta_{sol}H$, of four common salt solutions are shown in Fig. 4 a). The subscript of "sol" in front of H indicates that $\nu\Delta_{sol}H$ is the enthalpy of the system at that charge activity so that we refer $\nu\Delta_{sol}H$ as enthalpy here on in. The enthalpy has a tendence to decrease with concentration. At 0.0001 M, KCl solution has an enthalpy 41.31 mJ/mol. At 5 M, it reduced to 6.4 mJ/mol. For KNO_3 solutions, the enthalpy is 50.82 mJ/mol at 0.0001 M and 31.34 mJ/mol at 5 M. NaCl has the lowest enthalpy, it is 11.91 mJ/mol at 0.0001 M and becomes negative value from 3 M. At 5 M it is −65.47 mJ/mol. For $NaNO_3$ solutions, its enthalpy is 3.58 mJ/mol at 0.0001 M and − 3.28 at 5 M. The results indicate that salt dissolution needs to absorb more heat at lower concentration but absorb less heat at higher concentration. Negative enthalpy values for both NaCl and $NaNO_3$ at higher concentration mean salt dissolution is releasing heat. The reason behind the phenomenon might be that at higher concentration, the particles in the solution have more chances to collide with each other and thus the heat is generated during the collisions. The heat absorbed or released during the experiments were not measured since the resource was not available at the time in the laboratory to measure the heat transfer accurately.

The product of charge activity and entropy, $\nu\Delta S$ of four common salt solutions are shown in Fig. 4 b). For the same reason as $\nu\Delta_{sol}H$, we name $\nu\Delta S$ as entropy. Entropies are much smaller than those of enthalpies. For example, enthalpy of KNO_3 solution at 6 M is 31.34 mJ/mol but the entropy of it is only 0.15 mJ/mol. Entropy decreased with concentration. For KCl solutions, entropy is 0.20 mJ/mol at 0.0001 mol/L and it deceases to 0.03 mJ/mol at 6 M. The entropy of KNO_3 is 0.25 mJ/mol at 0.0001 M and 0.15 mJ/mol at 6 M. For NaCl solutions, its entropy is 0.05 mJ/mol at 0.0001 M and it becomes negative values from 3 M. At 5 M it is −0.10 mJ/mol. The entropy of $NaNO_3$ is 0.16 mJ/mol at 0.0001 M and − 0.01 mJ/mol at 5 M. The results show that at lower salt concentrations particles in solutions are more chaotic and at higher concentrations particles become less chaotic and more orderly. This might be due to that salt particles at higher concentration tend to collide more and have more tendency to aggregate.

In this study, the investigation of common salts revealed a consistent relationship between changes in thermodynamic properties (enthalpy, Gibbs energy and entropy) and pH (Fig. 5). The results demonstrated that all the common salts exhibited similar behavior, thereby confirming the utility of pH as a reliable indicator for obtaining accurate thermodynamic properties of the salts under investigation.

Currently, the literature provides molar enthalpy values solely for chemicals with an ionic number of 1. However, in order to calculate their entropies and explore the relative disorder of compounds with ionic numbers greater than one, it is crucial to obtain the molar enthalpy values for these compounds. This endeavor will uncover fascinating insights and reveal intriguing facts about their thermodynamic properties.

4. Conclusions

The pH of an aqueous system is used as a measure of hydrogen-ion activity of solutions which equals to the charge activity. Electrostatic potentials are converted from measured pH values using Nernst equation. The product of charge activity and electrostatic potential is the potential energy of a system, which is related to Gibbs energy in thermodynamics. This is the first time that charge activity, either v or -v, is used to obtain the values of Gibb's energy. This Gibb's energy aids in computing the entropy of an aqueous system. Thus, just measuring the pH, the entropy of an aqueous system can be computed. The results indicate that positively charged salt solutions (pH < 7) exhibit a reduced propensity to dissolve in water as the concentration is increased. Conversely, negatively charged salt solutions, such as NaCl, can exhibit enhanced solubility in water at higher salt concentrations exceeding 4 M. However, it is important to note that the extent of increased dissolution is constrained by the saturation point, beyond which further dissolution is limited. In this study, it was found that when the concentrations of NaCl, KCl, $NaNO_3$ and KNO_3 increased in single solutions the entropies of those solutions tend to decrease allowing them to achieve orderly states. Sodium salts tend to reach the orderly state at lower concentrations compared to the potassium salts.

CRediT authorship contribution statement

Li Shu: Conceptualization, Methodology, Validation, Investigation, Resources, Writing – original draft, Writing – review & editing, Supervision, Project administration, Funding acquisition. **Veeriah Jegatheesan:** Resources, Writing – review & editing, Funding acquisition. **Leonardo Jegatheesan:** Writing – review & editing.

Declaration of competing interest

The authors of this manuscript have no conflict interest in publishing this manuscript.

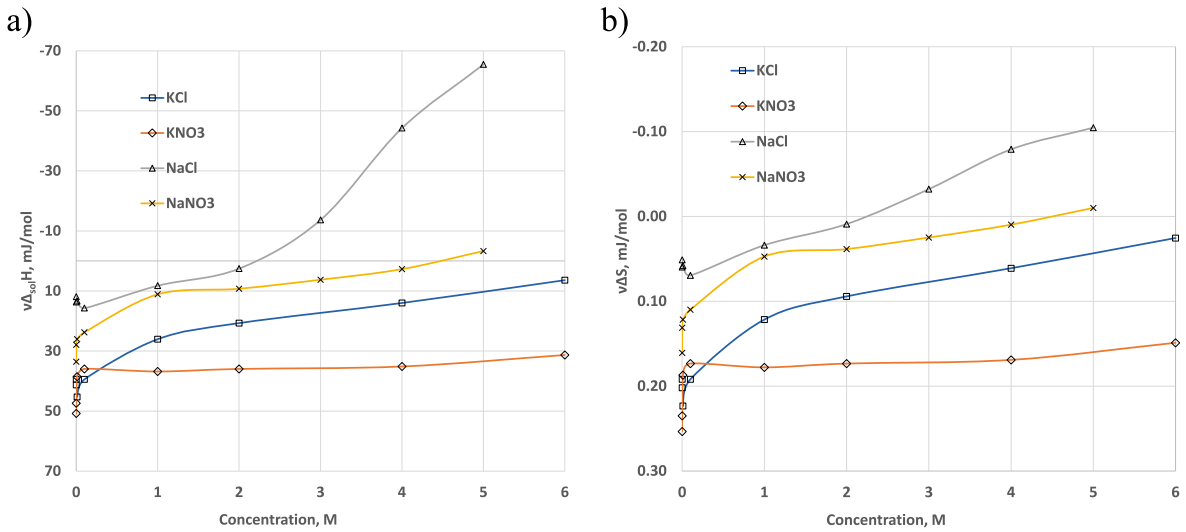

Fig. 4. Enthalpy and entropy of the four common salts studied.

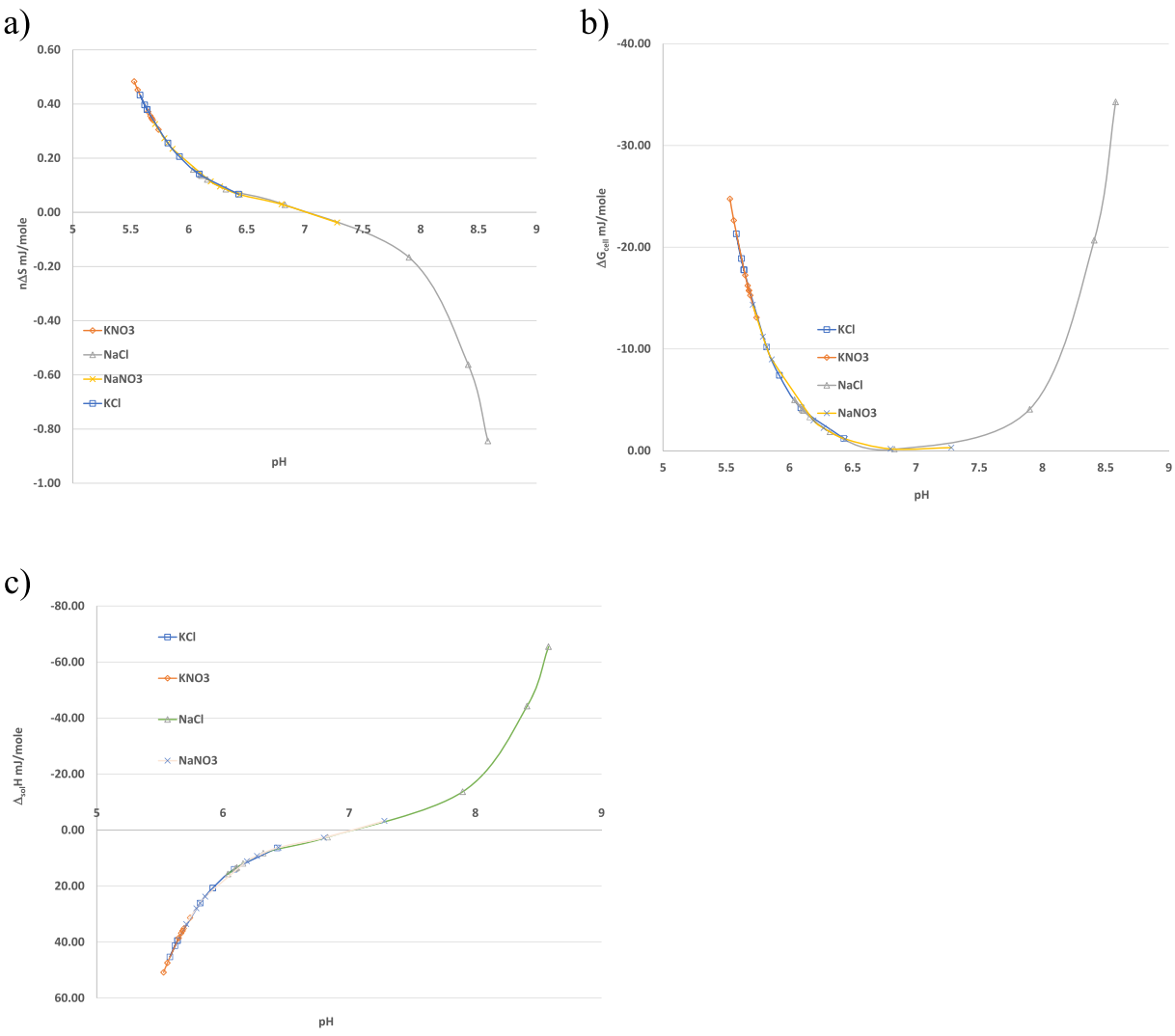

Fig. 5. Relationship between the thermodynamic properties and pH of the common salt solutions: a) Enthalpy; b) Gibbs energy and c) Entropy.

Data availability

Data will be made available on request.

Acknowledgement

Authors thank Jane (Xiujuan) Dai, Qiang Zhang and Rongli Xu for the discussion; Xi Lu and Qingyu Zhu for analysing pHs of potassium and sodium salts respectively and thanks to the management and staff, especially Steve Bagshaw and Leanne Farago at School of Engineering, Deakin University, for the financial and technical support to the research.

References

[1] M. Ayaz, M.A. Namazi, M. Ammad ud Din, M.I.M. Ershath, A. Mansour, e.-HM. Aggoune, Sustainable seawater desalination: current status, environmental implications and future expectations, Desalination 540 (2022), 116022.
[2] I. Ihsanullah, M.A. Atieh, M. Sajid, M.K. Nazal, Desalination and environment: a critical analysis of impacts, mitigation strategies, and greener desalination technologies, Sci. Total Environ. 780 (2021), 146585.
[3] E. Jones, M. Qadir, M.T.H. van Vliet, V. Smakhtin, S.-m. Kang, The state of desalination and brine production: a global outlook, Sci. Total Environ. 657 (2019) 1343–1356.
[4] A. Kumar, G. Naidu, H. Fukuda, F. Du, S. Vigneswaran, E. Drioli, J.H. Lienhard V, Metals recovery from seawater desalination brines: technologies, opportunities, and challenges, ACS Sustain. Chem. Eng. 9 (2021) 7704–7712.
[5] A. Ali, C.A. Quist-Jensen, M.K. Jørgensen, A. Siekierka, M.L. Christensen, M. Bryjak, C. Hélix-Nielsen, E. Drioli, A review of membrane crystallization, forward osmosis and membrane capacitive deionization for liquid mining, in: Resources, Conservation & Recycling 168, 2021, p. 105273.
[6] P. Loganathan, G. Naidu, S. Vigneswaran, Mining valuable minerals from seawater: a critical review, Environ. Sci. Water Res. Technol. 3 (2017) 37–53.
[7] M.O. Mavukkandy, C.M. Chabib, I. Mustafa, A.A. Ghaferi, F. AlMarzooqi, Brine management in desalination industry: from waste to resources generation, Desalination 472 (2019), 114187.
[8] O. Ogunbiyi, J. Saththasivam, D. Al-Masri, Y. Manawi, J. Lawler, X. Zhang, Z. Liu, Sustainable brine management from the perspectives of water, energy and mineral recovery: a comprehensive review, Desalination 513 (2021), 115055.
[9] C.A. Quist-Jensen, A. Ali, E. Drioli, F. Macedonio, Perspectives on mining from sea and other alternative strategies for minerals and water recovery - the development of novel membrane operations, J. Taiwan Inst. Chem. Eng. 94 (2019) 129–134.
[10] Q. Wang, E. Nakouzi, E.A. Ryan, C.V. Subban, Flow-assisted selective mineral extraction from seawater, Environ. Sci. Technol. Lett. 9 (2022) 645–649.
[11] T. Cho, M.-J. Kim, Synthesis of magnesium sulfate from seawater using alkaline industrial wastes, sulfuric acid, and organic solvents, Sep. Sci. Technol. 54 (2019) 2749–2757.
[12] K. Ghyselbrecht, B. Sansen, A. Monballiu, Z.-L. Ye, L. Pinoy, B. Meesschaert, Cationic selectrodialysis for magnesium recovery from seawater on lab and pilot scale, Sep. Purif. Technol. 221 (2019) 12–22.
[13] T. Dong, J. Yao, Y. Wang, T. Luo, L. Han, On the permselectivity of di-and mono-valent cations: influence of applied current density and ionic species concentration, Desalination 488 (2020), 114521.
[14] J. Liao, Q. Chen, N. Pan, X. Yu, X. Gao, J. Shen, C. Gao, Amphoteric blend ion-exchange membranes for separating monovalent and bivalent anions in electrodialysis, Sep. Purif. Technol. 242 (2020), 116793.
[15] W. Wang, R. Liu, M. Tan, H. Sun, Q.J. Niu, T. Xu, V. Nikonenko, Y. Zhang, Evaluation of the ideal selectivity and the performance of selectrodialysis by using TFC ion exchange membranes, J. Membr. Sci. 582 (2019) 236–245.

[16] Y. Yang, Y. Sun, X. Song, J. Yu, Separation of mono-and di-valent ions from seawater reverse osmosis brine using selective electrodialysis, Environ. Sci. Pollut. Res. 28 (2021) 18754–18767.
[17] Y.-F. Zhang, L. Liu, J. Du, R. Fu, B. Van der Bruggen, Y. Zhang, Fracsis: ion fractionation and metathesis by a NF-ED integrated system to improve water recovery, J. Membr. Sci. 523 (2017) 385–393.
[18] Z.-L. Ye, K. Ghyselbrecht, A. Monballiu, T. Rottiers, B. Sansen, L. Pinoy, B. Meesschaert, Fractionating magnesium ion from seawater for struvite recovery using electrodialysis with monovalent selective membranes, Chemosphere 210 (2018) 867–876.
[19] J.-H. Bang, S.-C. Chae, K. Song, S.-W. Lee, Optimizing experimental parameters in sequential CO_2 mineralization using seawater desalination brine, Desalination 519 (2022), 115309.
[20] W.Y. Choi, C. Aravena, J. Park, D. Kang, Y. Yoo, Performance prediction and evaluation of CO_2 utilization with conjoined electrolysis and carbonation using desalinated rejected seawater brine, Desalination 509 (2021), 115068.
[21] J. Lim, D.J. Kim, H. Cho, J. Kim, Design of novel seawater bittern recovery process for CO_2 and SOx utilization, Desalination 540 (2022), 115995.
[22] X. Zhang, W. Zhao, Y. Zhang, V. Jegathesan, A review of resource recovery from seawater desalination brine, Rev. Environ. Sci. Biotechnol. 20 (2021) 333–361.
[23] R. Bouchrit, A. Boubakri, T. Mosbahi, A. Hafiane, Sal-T Bouguecha, Membrane crystallization for mineral recovery from saline solution: study case Na_2SO_4 crystals, Desalination 412 (2017) 1–12.
[24] B. Chen, C. Jiang, Y. Wang, R. Fu, Z. Liu, T. Xu, Selectrodialysis with bipolar membrane for the reclamation of concentrated brine from RO plant, Desalination 442 (2018) 8–15.
[25] Y. Choi, G. Naidu, S. Jeong, S. Lee, S. Vigneswaran, Effect of chemical and physical factors on the crystallization of calcium sulfate in seawater reverse osmosis brine, Desalination 426 (2018) 78–87.
[26] H. Dong, C. Unluer, E.-H. Yang, A. Al-Tabbaa, Recovery of reactive MgO from reject brine via the addition of NaOH, Desalination 429 (2018) 88–95.
[27] N. Mahmud, D.V.F. Alvarez, M.H. Ibrahim, M.H. El-Naas, D.V. Esposito, Magnesium recovery from desalination reject brine as pretreatment for membraneless electrolysis, Desalination 525 (2022), 115489.
[28] C. Morgante, F. Vassallo, G. Battaglia, A. Cipollina, F. Vicari, A. Tamburini, G. Micale, Influence of operational strategies for the recovery of magnesium hydroxide from brines at a pilot scale, Ind. Eng. Chem. Res. 61 (2022) 15355–15368.
[29] F. Du, D.M. Warsinger, T.I. Urmi, G.P. Thiel, A. Kumar, J.H. Lienhard V, Sodium hydroxide production from seawater desalination brine: process design and energy efficiency, Environ. Sci. Technol. 52 (2018) 5949–5958.
[30] A. Kumar, K.R. Phillips, J. Cai, U. Schrçder, J.H. Lienhard V, Integrated valorization of desalination brine through NaOH recovery: opportunities and challenges, Angew. Chem. Int. Ed. 58 (2019) 6502–6511.
[31] M. Figueira, M. Reig, M.F. de Labastida, J.L. Cortina, C. Valderrama, Boron recovery from desalination seawater brines by selective ion exchange resins, J. Environ. Manag. 314 (2022), 114984.
[32] J. Li, R.R. Gonzales, R. Takagi, X. Yao, P. Zhang, T. Istirokhatun, J. Zhang, H. Matsuyama, Surface modification of thin film composite forward osmosis membrane using tris(2-aminoethyl)amine for enhanced ammonium recovery, Desalination 541 (2022), 116002.
[33] F. Arroyo, J. Morillo, J. Usero, D. Rosadob, H.E. Bakouri, Lithium recovery from desalination brines using specific ion-exchange resins, Desalination 468 (2019), 114073.
[34] G. Battaglia, L. Berkemeyer, A. Cipollina, J.L. Cortina, M.F. de Labastida, J. L. Rodriguez, D. Winter, Recovery of lithium carbonate from dilute Li-rich brine via homogenous and heterogeneous precipitation, Ind. Eng. Chem. Res. 61 (2022) 13589–13602.
[35] A.S. Bello, N. Zouari, D.A. Da'ana, J.N. Hahladakis, M.A. Al-Ghouti, An overview of brine management: emerging desalination technologies, life cycle assessment, and metal recovery methodologies, J. Environ. Manag. 288 (2021), 112358.
[36] D. İpekçi, N. Kabay, S. Bunania, E. Altıoka, M. Arda, K. Yoshizuka, S. Nishihama, Application of heterogenous ion exchange membranes for simultaneous separation and recovery of lithium and boron from aqueous solution with bipolar membrane electrodialysis (BMED), Desalination 479 (2020), 114313.
[37] S.Y. Jung, H. Joo, J.H. Kim, S. Kim, S. Heo, J. Yoon, Electrode design and performance of flow-type electrochemical lithium recovery (ELR) systems, Desalination 532 (2022), 115732.
[38] A. Khalil, S. Mohammed, R. Hashaikeh, N. Hilal, Lithium recovery from brine: recent developments and challenges, Desalination 528 (2022), 115611.
[39] S. Kim, H. Joo, T. Moon, S.H. Kim, J. Yoon, Rapid and selective lithium recovery from desalination brine using an electrochemical system, Environ Sci Process Impacts 21 (2019) 667–676.
[40] D.-H. Lee, T. Ryu, J. Shin, J.C. Ryu, K.-S. Chung, Y.H. Kim, Selective lithium recovery from aqueous solution using a modified membrane capacitive deionization system, Hydrometallurgy 173 (2017) 283–288.
[41] D. Liu, Z. Zhao, W. Xu, J. Xiong, L. He, A closed-loop process for selective lithium recovery from brines via electrochemical and precipitation, Desalination 519 (2022), 115302.
[42] G. Naidu, S. Jeong, M.A.H. Johir, A.G. Fane, J. Kandasamy, S. Vigneswaran, Rubidium extraction from seawater brine by an integrated membrane distillation-selective sorption system, Water Res. 123 (2017) 321–331.
[43] P. Ortiz-Albo, S. Torres-Ortega, M.G. Prieto, A. Urtiaga, R. Ibañez, Techno-economic feasibility analysis for minor elements valorization from desalination concentrates, Sep. Purif. Rev. 48 (2019) 220–241.
[44] B.K. Pramanik, L. Shu, V. Jegatheesan, A review of the management and treatment of brine solutions, Environ. Sci. Water Res. Technol. 3 (2017) 625–658.
[45] A. Werner, A. Rieger, K. Helbig, B. Brix, J. Zocher, R. Haseneder, J.-U. Repke, Nanofiltration for the recovery of indium and germanium from bioleaching solutions, Sep. Purif. Technol. 224 (2019) 543–552.
[46] P. Xing, C. Wang, Y. Chen, B. Ma, Rubidium extraction from mineral and brine resources: a review, Hydrometallurgy 203 (2021), 105644.
[47] Y. Zhang, Y. Hu, N. Sun, S.A. Khoso, L. Wang, W. Sun, A novel precipitant for separating lithium from magnesium in high Mg/Li ratio brine, Hydrometallurgy 187 (2019) 125–133.
[48] B.A. Sharkh, A.A. Al-Amoudi, M. Farooque, C.M. Fellows, S. Ihm, S. Lee, S. Li, N. Voutchkov, Seawater desalination concentrate-a new frontier for sustainable mining of valuable minerals, NPJ. Clean Water 5 (2022) 9, https://doi.org/10.1038/s41545-022-00153-6.
[49] A. Ghalavand, M.S. Hatamipour, Y. Ghalavand, Clean treatment of rejected brine by zero liquid discharge thermal desalination in Persian Gulf countries, Clean Techn. Environ. Policy 23 (2021) 2683–2696.
[50] A. Giwa, V. Dufour, F.A. Marzooqi, M.A. Kaabi, S.W. Hasan, Brine management methods: recent innovations and current status, Desalination 407 (2017) 1–23.
[51] K.G. Nayar, J. Fernandes, R.K. McGovern, B.S. Al-Anzi, J.H. Lienhard V, Cost and Energy Needs of RO-ED-crystallizer Systems for Zero Brine Discharge Seawater Desalination 457, 2019, pp. 115–132.
[52] R. Coterillo, L.-E. Gallart, E. Fernandez-Escalante, J. Junquera, P. García-Fernandez, I. Ortiz, R. Ibanez, M.-F. San-Roman, Selective extraction of lithium from seawater desalination concentrates: study of thermodynamic and equilibrium properties using Density Functional Theory (DFT), Desalination 532 (2022), 115704.
[53] K.M. Shah, I.H. Billinge, X. Chen, H. Fan, Y. Huang, R.K. Winton, N.Y. Yip, Drivers, challenges, and emerging technologies for desalination of high-salinity brines: a critical review, Desalination 538 (2022), 115827.
[54] I. Shefer, O. Peer-Haim, R. Epsztein, Limited ion-ion selectivity of salt-rejecting membranes due to enthalpy-entropy compensation, Desalination 541 (2022), 116041.
[55] W.M. Haynes, CRC Handbook of Chemistry and Physics, CRC Press, 2016.
[56] L. Shu, X. Lu, V. Jegatheesan, L. Jegatheesan, Investigating pH and other electrical properties of potassium salt solutions, Food Chem. Adv. 2 (2023), 100210.
[57] P. Atkins, J. de Paula, Atkin's Physical Chemistry, 10th ed., Oxford University Press, 2014.
[58] L. Shu, I.J. Obagbemi, S. Liyanaarachchi, D. Navaratna, R. Parthasarathy, R. Ben Aim, V. Jegatheesan, Why does pH increase with $CaCl_2$ as draw solution during forward osmosis filtration, Process. Saf. Environ. Prot. 104 (2016) 465–471.
[59] Shu L.J. Jegatheesan, V. Jegatheesan, C.Q. Li, The structure of water, Fluid Phase Equilib. 511 (2020), 112514.